J Nanopart Res (2017) 19: 1
DOI 10.1007/s11051-016-3643-3

RESEARCH PAPER

Unusual attempt to direct the growth of bimetallic Ag@Pt nanorods on electrochemically reduced graphene oxide nanosheets by electroless exchange of Cu by Pt for an efficient alcohol oxidation

S. E. Jeena · P. Gnanaprakasam · T. Selvaraju

Received: 16 July 2016 / Accepted: 23 October 2016 / Published online: 20 December 2016

Abstract A simple and an efficient tool for the direct growth of bimetallic Ag@Pt nanorods (NRDs) on electrochemically reduced graphene oxide (ERGO) nanosheets was developed at glassy carbon electrode (GCE). Initially, Cu shell was grown on Ag core as Ag@Cu NRD by the seed-mediated growth method. Accordingly, Cu shell has been successfully replaced by Pt using the electroless galvanic replacement method with ease by effective functionalization of L-tryptophan on ERGO surface (L-ERGO), which eventually plays an important role in the direct growth of one-dimensional bimetallic NRDs. As a result, the synthesized Ag@Pt NRD-supported L-ERGO nanosheets (Ag@Pt NRDs/L-ERGO/GCE) were characterized by scanning electron microscopy (SEM), X-ray diffraction (XRD), energy-dispersive X-ray analysis (EDAX) and Raman spectroscopy. Anodic stripping voltammetry was used to explore its electrochemical properties. Finally, the developed bimetallic Ag@Pt NRDs/L-ERGO/GCEs were studied as a better electrocatalyst compared to the commercial catalysts such as Pt_{40}/C or Pt_{20}/C-loaded electrode for the oxidation of ethanol or methanol with a high tolerance level and an enhanced current density. In addition, the long-term stability was studied using chronoamperometry for 1000 s at the bimetallic NRD electrode for alcohol oxidation which impedes the fouling properties. The unfavourable and favourable electrooxidation of ethanol at Ag@Cu NRDs/L-ERGO/GCE (a) and Ag@Pt NRDs/L-ERGO/GCE (b) is discussed. The synergistic effect of Ag core and catalytic properties of Pt shell at Ag@Pt NRDs/L-ERGO/GCE tend to strongly minimize the CO poisoning effect and enhanced ethanol electrooxidation.

Keywords Electrochemically reduced graphene oxide-modified electrodes · Bimetallic Ag@Pt nanorods · Seed-mediated growth process · Galvanic replacement · Methanol oxidation · Ethanol oxidation

S. E. Jeena · P. Gnanaprakasam
Department of Chemistry, Karunya University, Coimbatore 641 114, India

T. Selvaraju (✉)
Department of Chemistry, Bharathiar University, Coimbatore 641 046, India
e-mail: veluselvaraju@gmail.com

Introduction

Recent scientific community pave a great interest in exploring noble metal nanostructures due to their high efficiency in different fields such as fuel cells, optics, electronics and chemical sensors (Meir et al. 2013; Xu et al. 2011; Tedsree et al. 2011). Its catalytic property is closely related to their composition, morphology and dimension. Among the noble metals, nanostructured Pt catalysts are extensively studied in fuel cell applications (He et al. 2010a,b; Divya and Ramaprabhu 2013). However, the major challenges in developing Pt catalysts that are high cost, kinetic limitation of oxygen reduction and rapid poisoning due to CO-like intermediate species generation would affect the efficiency of direct alcohol fuel cells (DAFCs) (Chen and Hindle 2010; Zeng et al. 2006). Bimetallic Pt nanostructures such as core-shell or

alloys with other metals like Ru, Rh, Au and Ag tend to resolve the drawback and enhanced its catalytic activity (Zeng et al. 2006; Liu et al. 2014; Du et al. 2012; Cheng et al. 2014). Zhang et al. designed Pt shell nanoparticles with alloy core for oxygen reduction reaction (Zhang et al. 2013). Liu et al. demonstrated the design and preparation of stellated Ag-Pt bimetallic nanoparticles for methanol oxidation and oxygen reduction reaction (Liu et al. 2014).

Carbon materials such as carbon black, carbon nanotubes and carbon nanofibers were widely used as supporting material for Pt catalysts to improve its catalytic efficiency (Maiyalagan et al. 2012; Nguyen et al. 2013; Xi et al. 2007). Among carbon materials, graphene oxide nanosheets have been considered as better supporting material for Pt catalysts due to its high surface area, enhanced mechanical strength and good thermal and electrical conductivity (Sharma et al. 2010; Wang et al. 2014; Shen et al. 2014). Feng et al. synthesized Pt–Ag alloy nanoisland/graphene hybrid composites to study its electrocatalytic activity towards methanol oxidation (Feng et al. 2011). Cui et al. deposited Au@Pt core-shell nanoparticles on the reduced graphene oxide surface and used for methanol oxidation (Cui et al. 2013). Even though the incorporation of metal nanostructures on the graphene oxide surface was widely reported (Liu et al. 2012; Lee et al. 2013; Luo et al. 2012a,b; Zeng et al. 2015; Luo et al. 2012a,b), the direct growth of bimetallic NRDs or nanowires on reduced graphene oxide surface is not yet investigated effectively. In the present investigation, an effective method for the direct growth of bimetallic Ag@Pt NRDs on L-ERGO/glassy carbon electrode (GCE) surface is introduced where bimetallic Ag@Cu NRDs are grown on L-ERGO nanosheets by simple seed-mediated growth method followed by replacing the Cu shell by Pt through electroless galvanic replacement method. Recently, the first stage of direct growth of bimetallic Ag@Cu NRDs on L-ERGO nanosheets was established and reported elsewhere (Jeena et al. 2015).

In general, the synthesis of Ag-based bimetallic alloy or core-shell nanostructures was either reported by the simultaneous co-reduction of two different metal atoms or by the successive reduction of one metal over the seed of other metal (Chen et al. 2007; He et al. 2010a,b; Wojtysiak et al. 2014). On the other hand, the electroless galvanic replacement method has proved as a simple and an efficient tool to develop a thin layer of shell-like nanostructures of any noble metal catalysts using an extremely low proportion of precursors (Zhang et al. 2012; Gnanaprakasam et al. 2015). Importantly, the difference in standard reduction potential between the metals is the driving force for the galvanic replacement reaction. Very few reports have shown the formation of bimetallic Ag@Pt nanostructures by a galvanic replacement method where Ag was used as the sacrificial template for the replacement process (Rashid et al. 2015; Chen et al. 2005). Accordingly, the direct Pt layer generation over an Ag surface by galvanic replacement was discontinuous due to the stripping of relatively large amount of Ag and alters its crystal structure and composition during Ag–Pt alloy nanostructure formation (Wojtysiak et al. 2014). The stripped Ag^+ ions in the replacement process have the tendency to precipitate as AgCl in the aqueous medium of Pt precursor and eventually would passivate the electrode surface. Therefore, the successful generation of bimetallic nanostructures at the electrode surface was affected (Xie et al. 2012). Ultimately to overcome these challenges, in the present work, the metallic Cu surface was introduced as a sacrificial template over Ag nanorods for the galvanic replacement reaction. Here, the exchanged Cu as Cu^{2+} will remain in the solution in an ionic state without forming any precipitate during the replacement process. In addition, the standard reduction potential of Cu^{2+}/Cu (0.34 V) is less compared to Ag^+/Ag (0.8 V) which enables the electroless galvanic replacement process of Pt layer at Ag NRDs. To the best of our knowledge, there is no report existing for the one-dimensional growth of Ag@Pt NRDs on an electrochemically reduced graphene oxide surface by Cu as a sacrificial template using the electroless galvanic replacement method. Consequently, the present investigation would highlight the importance of using Cu as a sacrificial template for the successful growth of Ag@Pt NRDs on L-ERGO surface to sweep over the stripping phenomena of Ag^+ ions at the electrode surface.

In addition, the synergistic effect of Ag metal possesses better capabilities for enhancement in the CO tolerance and thereby exhibits an increased catalytic activity and stability of Pt-based catalysts (Feng et al. 2011; Peng et al. 2015). At the outset, these properties have enlightened us to develop an Ag-based bimetallic nanostructure such as Ag@Pt NRDs on L-ERGO/GCE surface for a better catalytic activity with high CO tolerance and stability towards methanol or ethanol oxidation. Very recently, Au@Pt bimetallic nanoparticles on chemically reduced graphene oxide surface were

studied for alcohol oxidation, which favours methanol rather than ethanol oxidation (Gnanaprakasam et al. 2015). Instead of Au core and chemically reduced graphene oxide synthesis, in the present investigation, Ag core metal is introduced at L-ERGO surface to develop the bimetallic Ag@Pt NRDs/L-ERGO/GCE and to explore its possibility towards ethanol or methanol oxidation. The replacement of base metal has altered and favoured the catalytic property of Pt surface for ethanol oxidation. Usually, the electrooxidation of ethanol is very complex due to the release of 12 electrons to split C–C bonds (Kakaei and Dorraji 2014). Ultimately, the tolerance level and the stability of the electrode will be affected. Thus, the presence of Ag as core metal with Pt would enhance the efficiency of the catalyst based on the d-band theory where the combination of Ag and Pt resulted in the shift of d-band centre of Pt which tends to increase the adsorption of hydroxyl ions on the metal surface (Safavi et al. 2013). In addition, the presence of Ag would activate the water molecules and enable to oxidize the adsorbed poisonous species which, in turn, liberates the active sites. Thus, Ag would act as a better base metal for the development of bimetallic nanostructures of noble metal catalysts for ethanol oxidation. The electrochemical behaviour of the fabricated electrodes was investigated by cyclic voltammetry (CV) and chronoamperometry. Accordingly, a new avenue has opened up in the field of direct growth of bimetallic NRDs on L-ERGO surface which would enhance the catalytic activity for the electrooxidation of ethanol. Further, the synthesized new generation catalyst could be used as a better electrode material in tuning the performance of fuel cells.

Experimental

Materials

L-tryptophan, sulphuric acid, hydrogen peroxide, copper nitrate, sodium nitrate, sodium borohydride and sodium hydroxide were obtained from Merck, India. Methanol, ethanol and cetyl trimethyl ammonium bromide (CTAB) were purchased from HiMedia, India. Graphite powder crystalline (300 mesh), Pt_{20}/C (35849, MFCD00011179) and Pt_{40}/C (42204, MFCD00011179) were obtained from Alfa Aesar, UK. Ascorbic acid, trisodium citrate, hexachloroplatinic acid and silver nitrate were purchased from Sigma-Aldrich, USA. All reagents were analytical graded and used without any purification process. All solutions were prepared using double-distilled water.

Characterizations

Bimetallic Ag@Pt NRDs were grown on L-ERGO-modified ITO surface for exploring its structural and morphological behaviour. Preceding the development process, the ITO plates were cleaned and pretreated with H_2O, H_2O_2 and NH_4OH with the ratio of 5:1:1. The surface morphology of Ag@Pt NRD-decorated L-ERGO nanosheets was confirmed by scanning electron microscopy (SEM) (VEGA 3 TESCAN, USA). X-ray diffraction (XRD) pattern and energy-dispersive X-ray analysis (EDAX) mapping analyses were used to confirm the presence of metallic Ag and Pt. XRD patterns were analysed using Shimadzu XRD 6000 (Japan). EDAX measurements were carried out using an energy-dispersive X-ray analyser (Bruker, Germany). The Raman spectra were recorded using the Horiba-Jobin (LabRAM HR).

Electrochemical measurements

All electrochemical investigations were performed with a three-electrode set-up in an electrochemical workstation using CHI 660D (CH Instruments, USA). GCEs were polished with alumina (0.3 μm) using Buehler cloth and sonicated in ethanol-water blend for 3 min. Ag@Pt NRDs/L-ERGO/GCEs were used as the working electrode. An Ag/AgCl filled with a saturated KCl and Pt wire was used as reference and counter electrodes, respectively.

Synthesis of Ag@Pt NRDs/L-ERGO nanosheets on GCE surface

Graphene oxide (GO) has been used as the basic material for the synthesis of ERGO-modified electrodes. GO was prepared by the modified Hummers method (Jeena et al. 2015; Gnanaprakasam and Selvaraju 2014). The prepared GO should be dispersed well in DI water under ultrasonication with a fine concentration of 0.3 mg ml^{-1} where it is stable for more than 7 months. Initially, 10 μl of GO dispersion was drop casted on GCE surface and dried at room temperature. GO was electrochemically reduced by 40 successive cycles in the potential range between 0.0 and −1.5 V in 0.05 M phosphate buffer (pH 5). A reduction peak has appeared at −1.2 V at first few cycles due to the reduction of oxygen moieties on the GO surface and disappeared subsequently which

indicates the complete reduction of GO. Further, for an effective functionalization, the ERGO-modified electrode was dipped in L-tryptophan (1 mg ml^{-1}) at room temperature for 24 h and dried.

Bimetallic Ag@Pt NRDs were grown on L-ERGO surface by a seed-mediated growth process followed by the galvanic replacement method. Initially, bimetallic Ag@Cu NRDs were grown on L-ERGO/GCE by the simple seed-mediated growth method. Subsequently, Cu shell at the bimetallic Ag@Cu NRDs was subjected to galvanically replace by Pt in order to form a thin layer of Pt on Ag surface. The detailed synthetic route of Ag@Cu NRDs on L-ERGO-modified electrodes by the modified seed-mediated growth method has been reported elsewhere (Jeena et al. 2015). Further, Ag@Cu NRD-decorated L-ERGO nanosheet-modified electrodes were dipped in 2.4 mM aqueous solution of hexachloroplatinic acid for 95 s for the complete galvanic replacement of Cu by Pt. Finally, the bimetallic NRD-decorated electrode should be denoted as Ag@Pt NRDs/L-ERGO/GCE.

Results and discussion

Surface and morphological studies

Scheme 1 summarizes the stepwise growth of bimetallic Ag@Pt NRDs on L-ERGO surface by seed-mediated growth followed by galvanic replacement method. It demonstrates the growth of Ag_{seeds} into bimetallic Ag@Cu NRDs followed by the electroless replacement of Cu by Pt at L-ERGO-modified electrodes. The difference in the standard reduction potential between Cu^{2+}/Cu ($E°$ = +0.34 V) and Pt^{4+}/Pt ($E°$ = +1.44 V) has accounted for the galvanic replacement reaction. Figure 1 shows the SEM images of ERGO (a) and bimetallic Ag@Pt NRDs (b) decorated L-ERGO nanosheets. Figure 1a displays the wrinkled morphology of ERGO nanosheets on the electrode surface, and Fig. 1b demonstrates the effective growth of bimetallic Ag@Pt NRDs at L-ERGO surface with the size distribution of 185 ± 2-nm diameter thickness and 1-μm length. The intermediate step of demonstrating SEM image of Ag@Cu NRDs at L-ERGO has been reported elsewhere (Jeena et al. 2015). In the present study, the shell-like Cu has replaced as a sacrificial template for the successful generation of a thin Pt layer over an Ag NRD surface by galvanic replacement. It seems to be an efficient route for the formation of a thin layer of noble metal nanostructures such as bimetallic or core-shell nano alloy-based NRDs. On the other hand, after galvanic replacement of Cu by Pt at the bimetallic NRD-decorated L-ERGO surface, no significant variation has been observed in the surface morphology or size distribution which is evidently confirmed by SEM analysis.

The existence of bimetallic such as Ag and Pt at Ag@Pt NRDs/L-ERGO was confirmed by EDAX

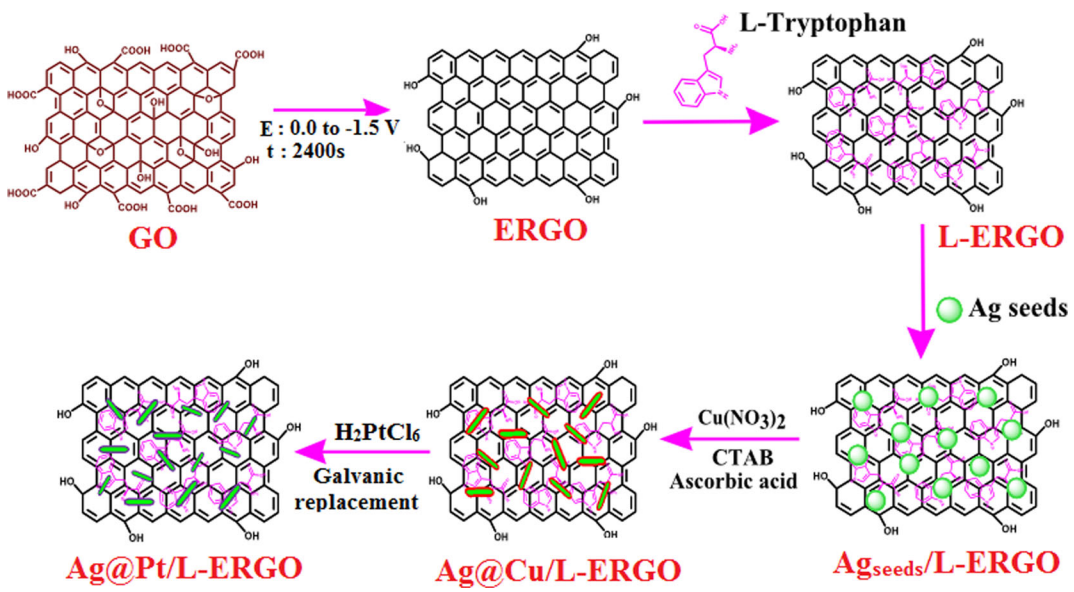

Scheme 1 Schematic representation for the stepwise growth of Ag_{seeds} into bimetallic Ag@Pt NRDs on L-ERGO nanosheets

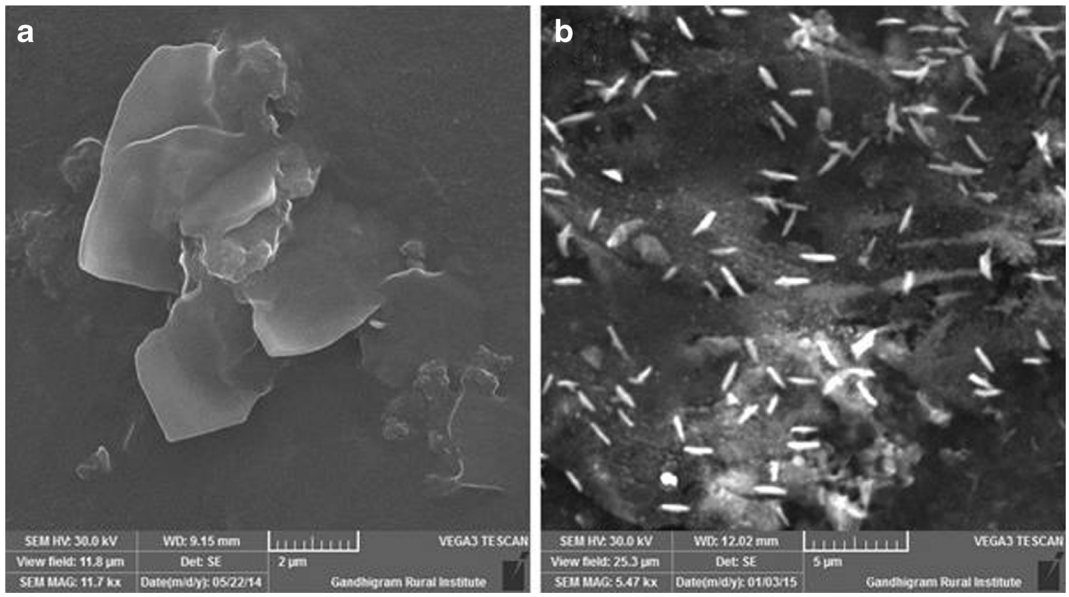

Fig. 1 SEM images of ERGO (**a**) and Ag@Pt NRDs/L-ERGO (**b**) on electrode surfaces

spectra and elemental mapping analysis. Figure 2 shows the elemental mapping analysis and the EDAX pattern of Ag@Pt NRDs/L-ERGO-modified electrodes. EDAX measurements of Ag@Cu NRDs/L-ERGO were reported elsewhere (Jeena et al. 2015). The result derived from Fig. 2 would substantiate the complete replacement of Cu by Pt through galvanic replacement. In addition, the XRD patterns have justified the existence of bimetallic Ag and Pt through the complete replacement of Cu at Ag@Pt NRDs/L-ERGO surfaces (Fig. 3). The diffraction pattern at 10.1° was minimized, and a new diffraction pattern was observed at 24.1° for ERGO which inferred the complete electrochemical reduction of graphene oxide. Besides, the XRD pattern of bimetallic Ag@Cu NRDs/L-ERGO (a) shows that peaks at 17.1°, 20.6° and 27.5° correspond to Ag and 20.6°, 23.5° and 38.2° correspond to Cu (Jeena et al. 2015). On the other hand, after Cu replacement by Pt, the diffraction pattern that corresponds to metallic Cu did completely disappeared and new diffraction patterns at 20.7° (2 0 0), 28.9° (2 2 0) and 36.3° (2 2 2) were observed which exhibits the presence of Pt at Ag@Pt NRDs/L-ERGO (b). In addition, the peaks at 21.7° and 31° correspond to ITO surface. Eventually, all the diffraction patterns were correlated with JCPDS nos. 011167 (Ag), 011311 (Pt) and 320458 (ITO), respectively. Thus, the XRD pattern has firmly validated the complete replacement of Cu by Pt and thereby the successful growth of Ag@Pt NRDs on L-ERGO surface by galvanic replacement reaction.

Raman spectra are extremely sensitive to electronic structure, and it is considered as an effective tool to characterize graphene-based materials. Figure 4 shows the Raman spectrum of Ag@Pt NRDs/L-ERGO-modified electrode. D and G bands at 1350 and 1590 cm^{-1} corresponds to the breathing mode of A_{1g} symmetry and first-order scattering of E_{2g} vibrational mode. The intensity ratio of D and G bands (I_D/I_G) has been considered as a degree of disorderness on the graphene nanosheets. Initially, I_D/I_G ratio was calculated as 1.42 for ERGO (Jeena et al. 2015). After the growth of bimetallic Ag@Cu NRDs on L-ERGO surface, the ratio has decreased to 1.03. It depicts the direct growth of Cu shell at Ag NRDs as Ag@Cu NRDs on L-ERGO surface (Jeena et al. 2015). Further, upon galvanic replacement of Cu by Pt at Ag@Pt NRDs/L-ERGO nanosheets, a slight increase in the I_D/I_G ratio to 1.15 is observed. It is due to an insignificant increase in the disorderness upon the generation of a thin layer of Pt at Ag NRD surface. The second-order band (2D) and the combination band (D + G) at 2680 and 2939 cm^{-1} are correlated with the graphitic phases of the nanosheets. The intensity of 2D band is an evidence for the generation of exfoliated graphene oxide at the electrode surface.

Electrochemical characterizations

CV studies have been considered as an effective surface sensitive tool which enables the electrochemical

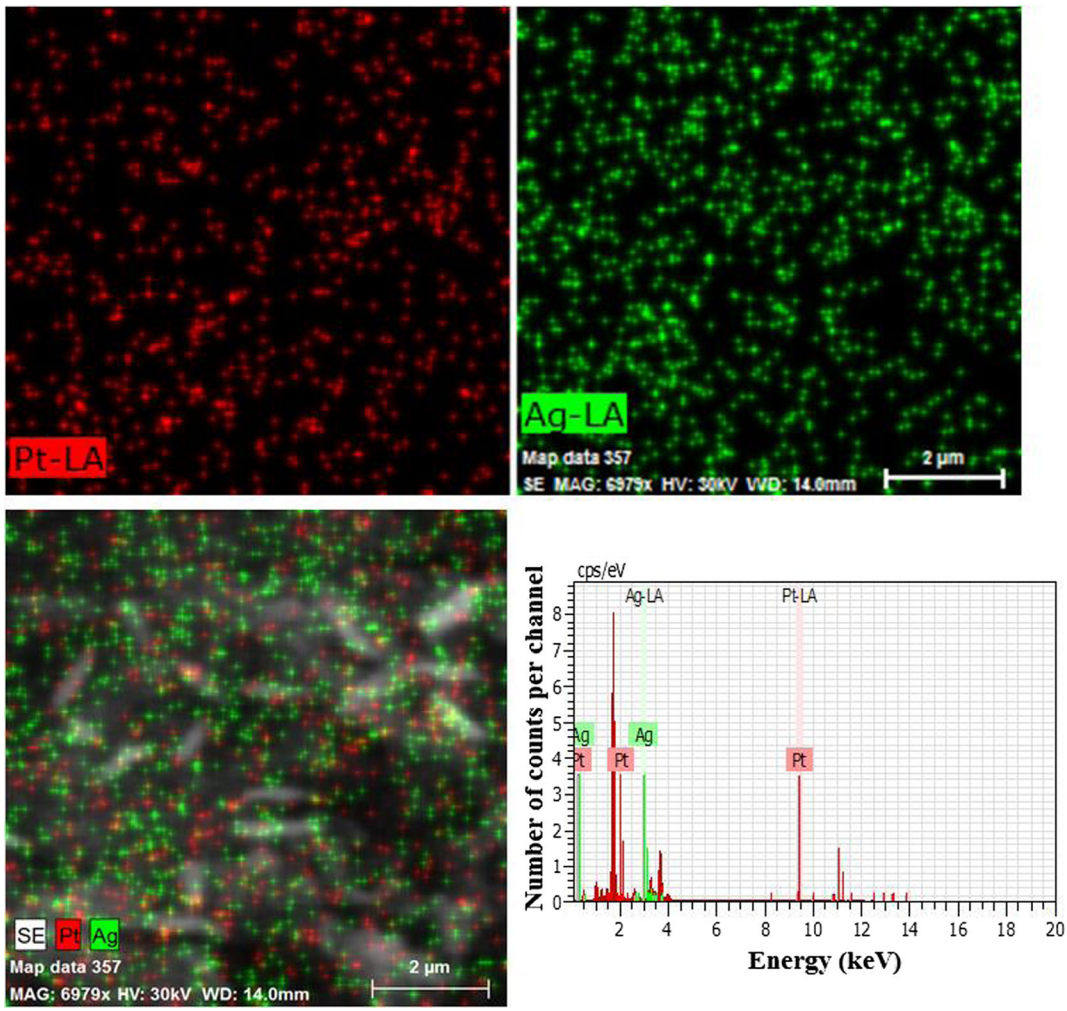

Fig. 2 EDAX spectra and elemental mapping analyses of bimetallic Ag@Pt NRDs/L-ERGO nanosheet-modified electrode

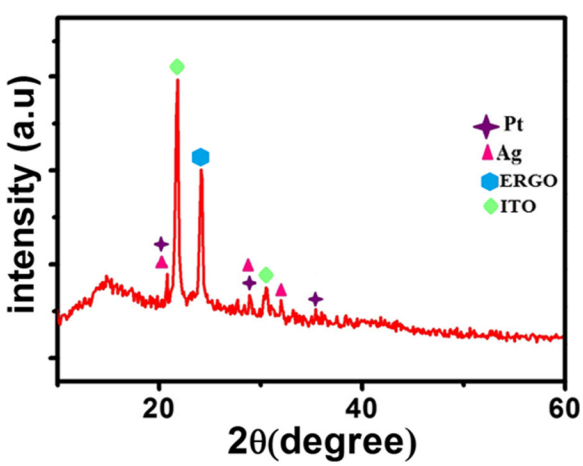

Fig. 3 XRD pattern of Ag@Pt NRDs/L-ERGO nanosheet-modified electrodes

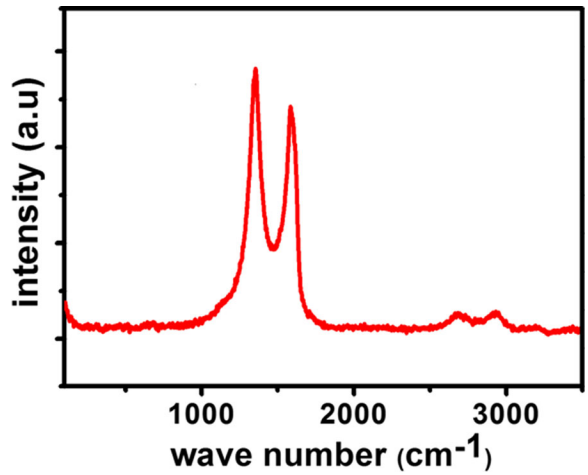

Fig. 4 Raman spectrum of Ag@Pt NRDs/L-ERGO nanosheet-modified electrodes

information of surface atoms compared to the bulk material. CV responses of Ag_{seeds}/L-ERGO/GCE and Ag@CuNRDs/L-ERGO/GCE were studied in N_2-saturated 0.5 M H_2SO_4 and reported elsewhere (Jeena et al. 2015). After electroless Cu replacement by Pt, the anodic stripping peak current that corresponds to Cu or Ag disappeared. Figure 5 shows a CV response of bimetallic Ag@Pt NRDs/L-ERGO/GCE in N_2-saturated 0.5 M H_2SO_4. It shows a broad oxidation and reduction waves in the range of −0.3 to 0.1 V corresponding to the hydrogen adsorption/desorption process which typically correlates the presence of Pt surface. Predominantly, there is no stripping behaviour at 0.23 V which was a solid evidence for the confinement of Ag dissolution (Jeena et al. 2015; Easow and Selvaraju 2013). In addition, CV results would validate the masking properties of thin Pt layer at the Ag NRD surface as bimetallic Ag@Pt NRDs on L-ERGO. This evidently confirmed the presence of Pt over an Ag surface at Ag@Pt NRDs/L-ERGO electrodes.

Electrocatalytic activities of Ag@Pt NRDs/L-ERGO/GCE

The electrocatalytic behaviour of bimetallic Ag@Pt NRDs/L-ERGO/GCE or commercial catalysts such as Pt_{40}/C or Pt_{20}/C-loaded electrodes was investigated for the oxidation of ethanol or methanol in alkaline media. Importantly, the number of catalytic active sites at different catalyst-loaded electrodes was determined using the electroactive surface area (ECSA). After double-layer correction, the ECSA has been estimated from the accumulated charge under the hydrogen adsorption/desorption process. It was studied using CV response at different catalyst-loaded electrodes in 0.1 M H_2SO_4 at a scan rate of 50 mV/s with the Eq. (1).

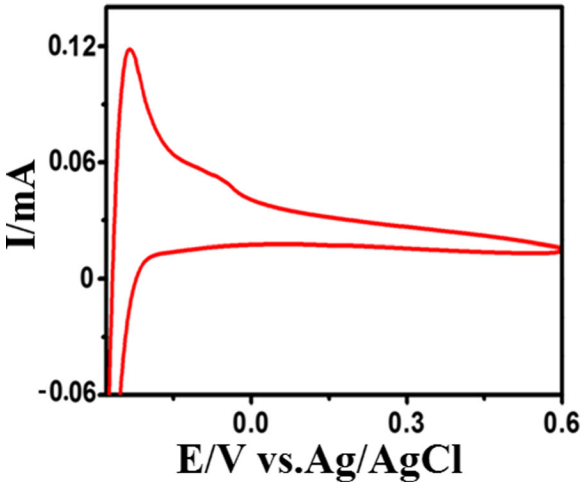

Fig. 5 Cyclic voltammetric response of Ag@Pt NRDs/L-ERGO/GCE in 0.5 M H_2SO_4 at a scan rate of 50 mV s^{-1}

$$\mathrm{ESCA} = \mathrm{Q_H} \Big/ \mathrm{Q_{H^*}} m \tag{1}$$

Here, Q_H is the charge associated with the hydrogen adsorption/desorption region, Q_{H*} is the charge density associated with the adsorption of hydrogen monolayer (210 μC cm^{-2}) and m is the mass of Pt loaded on the electrode. The calculated ECSA for the bimetallic Ag@Pt NRDs/L-ERGO/GCE or Pt_{20}/C or Pt_{40}/C-loaded electrodes is 53.5, 39.7 and 27.8 m^2 g_{pt}^{-1}, respectively. Thus, a thin layer of Pt generation via galvanic replacement process exhibits a high ECSA at bimetallic Ag@Pt NRDs/L-ERGO/GCE compared to other commercial high weight percentage catalysts such as 20% (Pt_{20}/C) or 40% (Pt_{40}/C) Pt-loaded electrodes.

The electrocatalytic activity of Ag@Pt NRDs/L-ERGO-modified electrode for ethanol or methanol oxidation was compared with Pt_{20}/C or Pt_{40}/C-loaded electrodes in terms of specific activity (current density normalized by surface area of the catalysts) and mass activity (current density normalized by the mass of Pt loaded). The mass of Pt at bimetallic Ag@Pt NRDs/L-ERGO was calculated from EDAX analysis or ICP-AES and compared with the commercial catalyst-loaded electrodes. It is calculated as 1.35, 12 and 24 μg cm^{-2} that correspond to bimetallic Ag@Pt NRDs/L-ERGO/GCE, Pt_{20}/C/GCE and Pt_{40}/C/GCE. Figure 6 shows the CV responses of bimetallic Ag@Pt NRDs/L-ERGO/GCE in terms of mass activity (a) and specific activity (b) for 0.5 M ethanol at the scan rate of 50 mV s^{-1}. The newly developed modified electrode exhibits an excellent electrooxidation of ethanol with ease at an anodic peak potential of −0.26 V with an onset potential at −0.72 V. Further, for comparison and in order to emphasize the importance of thin layer Pt generation at bimetallic NRD-decorated L-ERGO electrode, bare GCE (a), L-ERGO/GCE (b) and Ag@Cu NRDs/L-ERGO/GCE (c) were studied for the electrooxidation of ethanol under identical conditions (Fig. 6a (inset A)). Neither bare GCE nor bimetallic Ag@Cu NRD-decorated L-ERGO electrode had shown an observable oxidation current in the potential between −1.0 and 0.5 V. It validates the feasibility of ethanol oxidation at the Pt surface-loaded electrode rather than

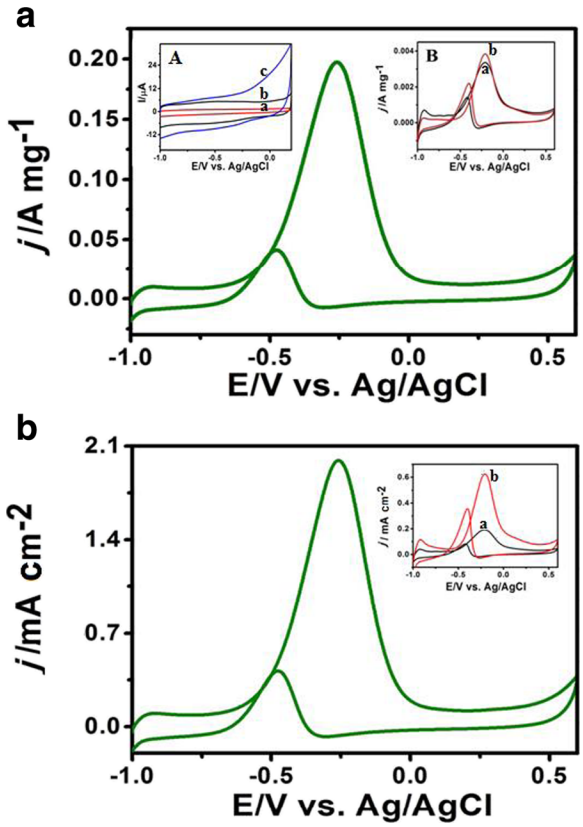

Fig. 6 CV response of mass activity (**a**) and specific activity (**b**) at Ag@Pt NRDs/L-ERGO/GCE for 0.5 M ethanol in 0.5 M NaOH at the scan rate of 50 mV s^{-1}. *Inset A* in **a** shows CVs of bare GCE (*a*), L-ERGO/GCE (*b*) and Ag@Cu NRDs/L-ERGO/GCE (*c*). *Inset B* in **a** and *inset* in **b** shows CVs of Pt_{20}/C/GCE (*a*) and Pt_{40}/C/GCE (*b*) for ethanol oxidation under identical conditions for mass activity and specific activity, respectively

at the Cu loaded or at bare electrode surfaces. Moreover, the electrocatalytic behaviour of bimetallic Ag@Pt NRDs/L-ERGO/GCE towards ethanol oxidation was compared with the commercial catalysts such as Pt_{20}/C or Pt_{40}/C-loaded electrodes in terms of its mass activity. Figure 6a (inset B) shows the CVs of Pt_{20}/C/GCE (a) or Pt_{40}/C/GCE (b) in 0.5 M ethanol under identical conditions where the onset potential and anodic peak potential were calculated as −0.54 and −0.2 V. On the other hand, Ag@Pt NRDs/L-ERGO/GCE exhibits a negative shift in both onset potential −0.72 V and anodic peak potential −0.26 V for ethanol oxidation. Thus, the developed catalyst exhibits 65 or 59 times higher mass activity compared to Pt_{20}/C or Pt_{40}/C commercial catalysts (Fig. 6a). Scheme 2 illustrates the unfavourable and the favourable condition for the electrooxidation of ethanol at Ag@Cu NRDs/L-ERGO/GCE (a) and Ag@Pt NRDs/L-ERGO/GCE (b), respectively. Though Pt surface possesses high catalytic activity for alcohol oxidation, the surface poisoning effect due to the generation of CO-like species is a main challenge. Ultimately, the generation of a thin layer of Pt at Ag surface as bimetallic Ag@Pt NRDs/L-ERGO electrode shows an enhancement in catalytic activity for ethanol oxidation with a high current density and reduced its surface poisoning effect. In CVs, the forward peak current (I_f) is responsible for the oxidation of ethanol and the backward peak current (I_b) is due to CO poisoning. The ratio of forward and backward peaks currents (I_f/I_b) is inversely proportional to the rate of intermediate adsorption. Thus, the ratio was calculated as 5 at Ag@Pt NRDs/L-ERGO/GCE towards electrooxidation of ethanol. It was very high compared to other commercial Pt

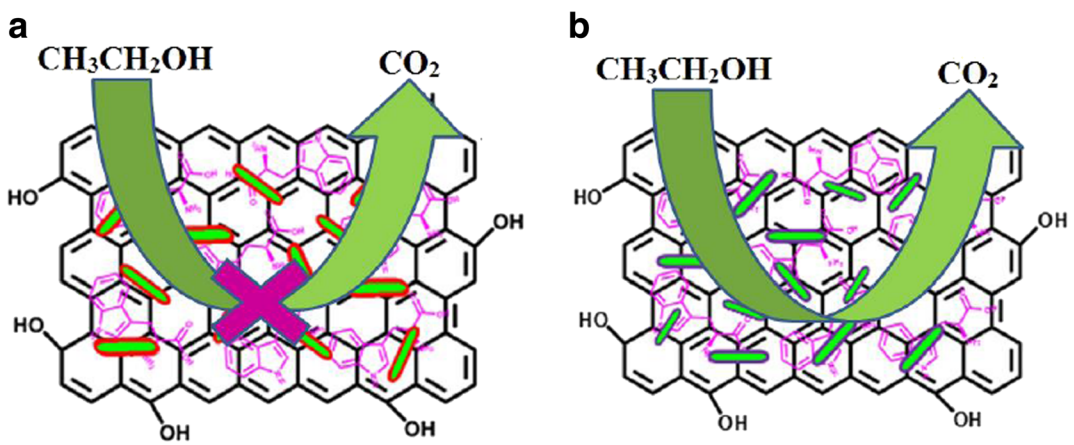

Scheme 2 Schematic representation of the electrooxidation of ethanol at Ag@Cu NRDs/L-ERGO/GCE (**a**) and Ag@Pt NRDs/L-ERGO/GCE (**b**)

Table 1 Comparison of onset potential (V), anodic peak potential (V), I_f/I_b ratio, specific activity (mA cm^{-2}) and mass activity (A mg^{-1}) of Ag@Pt NRDs/L-ERGO/GCE with commercial catalysts Pt_{20}/C/GCE and Pt_{40}/C/GCE for ethanol oxidation

Catalyst	Onset potential (V)	Anodic peak potential (V)	I_f/I_b	Specific activity (mA cm^{-2})	Mass activity (A mg_{pt}^{-1})
Ag@Pt/L-ERGO	−0.72	−0.26	5	2.0	0.19
Pt_{20}/C	−0.54	−0.2	1.8	0.19	0.0029
Pt_{40}/C	−0.54	−0.2	1.6	0.62	0.0032

catalyst-based electrodes (Gnanaprakasam et al. 2015) where a thin layer of Pt was generated at bimetallic NRDs as Ag@Pt at L-ERGO surface which exhibits a high tolerance ratio and better stability for the electrooxidation of ethanol. The weak chemisorptions of CO at Pt surface were closely associated with its high electron density. This factor had been overcome by the synergistic effect produced by the interaction between Ag and Pt at the bimetallic NRD electrode. The ligand effect and strain effect developed at the bimetallic Pt and Ag-based NRDs show better electron transfer kinetics. In addition, the ERGO nanosheet template provides a high surface area for favouring the electrooxidation of ethanol.

Moreover, the electrocatalytic behaviour of bimetallic Ag@Pt NRDs/L-ERGO/GCE towards ethanol oxidation was compared with the commercial catalysts such as Pt_{20}/C or Pt_{40}/C-loaded electrodes in terms of its specific activity (Fig. 6b). An enhanced current density of 10 or 3.2 times higher than Pt_{20}/C (Fig. 6b inset (a)) or Pt_{40}/C (Fig. 6b inset (b)) loaded electrodes was observed. Further, Ag@Pt NRDs/L-ERGO/GCE shows a high I_f/I_b ratio as 5 compared to 1.8 at Pt_{20}/C or 1.6 at Pt_{40}/C-loaded electrodes. Table 1 summarizes the onset potential, the anodic peak potential, the I_f/I_b ratio, the specific activity and the mass activity between the newly generated bimetallic and commercial catalyst-loaded electrodes. Finally, the high current density or high specific activity in terms of electrooxidation of ethanol at bimetallic Ag@Pt NRD-decorated L-ERGO electrode was observed due to the high efficiency of a thin layer of Pt generation via galvanic replacement reaction. In addition, the high I_f/I_b ratio was achieved due to the significant synergistic role of Ag as base metal at bimetallic NRDs which attributes to enhance the oxidation of CO-like poisonous species by imparting oxygen-containing species from aqueous media and thereby minimizing the poisoning level. Hence, the blending of bimetallic Ag@Pt NRDs at L-ERGO has allowed for the better electrooxidation of ethanol.

The long-term electrochemical stability of bimetallic Ag@Pt NRDs/L-ERGO/GCE for the electrooxidation of ethanol was investigated by chronoamperometry at −0.4 V for 1000 s (Fig. 7). Here, the current density has decreased rapidly at the initial stage due to the formation of the intermediate species, and after 400 s, a very minimum decrease in the current density up to 1000 s was observed. It indicates the better tolerance level and long-term stability of bimetallic Ag@Pt NRDs/L-ERGO electrodes. Compared to Pt_{20}/C or Pt_{40}/C-loaded electrodes, Ag@Pt NRDs/L-ERGO/GCE shows 22.9 or 7.6 times higher current density (Fig. 7 (inset)). In addition, the ratio of mass activity of the modified electrode has been calculated as 14.2 or 6.2 times higher than Pt_{20}/C or Pt_{40}/C-loaded electrodes. These results proved the unique bimetallic Ag@Pt NRD-decorated L-ERGO nanosheets as a better catalyst for the electrooxidation of ethanol with good stability and low poisoning effect.

Similarly, the electrocatalytic activity of bimetallic Ag@Pt NRDs/L-ERGO/GCE for methanol oxidation was compared with the commercial catalysts in terms

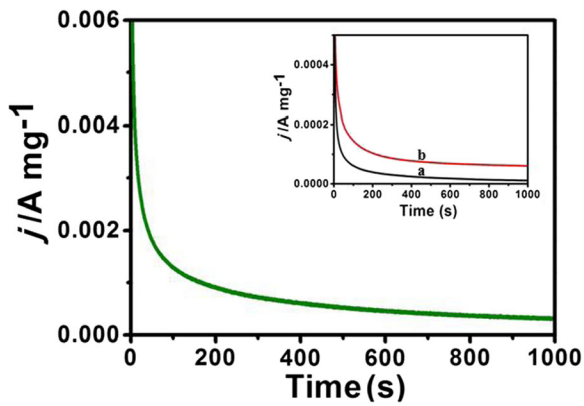

Fig. 7 CA curves of Ag@Pt NRDs/L-ERGO/GCE for 0.5 M ethanol in 0.5 M NaOH studied up to 1000 s at −0.4 V. The *inset* shows CA curves of Pt_{20}/C/GCE (*a*) and Pt_{40}/C/GCE (*b*) under identical conditions

of mass activity and specific activity. Figure 8 shows the CV response of Ag@Pt NRDs/L-ERGO/GCE in terms of mass activity (a) and specific activity (b) in 0.5 M methanol at the scan rate of 50 mV s^{-1}. It has shown an onset potential and an anodic peak potential at −0.5 and −0.24 V, respectively. Figure 8a solidly confirmed an enhanced catalytic activity at Ag@Pt NRDs/L-ERGO for methanol oxidation in terms of mass activity with a higher current density of 0.145 A mg_{pt}^{-1} compared to Pt_{20}/C (0.024 A mg_{pt}^{-1}) or Pt_{40}/C (0.016 A mg_{pt}^{-1}). Inset of Fig. 8a shows the CVs of Pt_{20}/C/GCE (a) and Pt_{40}/C/GCE (b) for methanol oxidation under identical conditions. Thus, the newly developed catalyst shows nine or six times higher efficiency compared to the commercial catalysts. Similarly, the specific activity of the catalyst for methanol oxidation was studied (Fig. 8b). It shows an electrooxidation of methanol with the current density 1.48 mA cm^{-2} which was comparable to Pt_{20}/C (Fig. 8b inset (a)) or Pt_{40}/C (Fig. 8b inset (b)) loaded electrode. Thus, the unique bimetallic NRDs on L-ERGO-decorated electrode exhibits a high tolerance level with the I_f/I_b ratio of 12 and low poisoning effect compared to the commercial Pt_{20}/C or Pt_{40}/C-loaded electrodes. The peak potential, the I_f/I_b ratio, the specific activity and the mass activity corresponding to different electrodes for methanol oxidation are tabulated in Table 2. Further, the electrochemical stability of bimetallic Ag@Pt NRDs/L-ERGO/GCE was studied for methanol oxidation by CA at −0.45 V for the period up to 1000 s (Fig. 9) and compared its efficiency with the commercial catalysts (Fig. 9 (inset)). In addition, the ratio of mass activity of the modified electrode was calculated as 1.2 or 1.77 times higher than Pt_{20}/C or Pt_{40}/C-loaded electrodes. The CA response of Ag@Pt NRDs/L-ERGO catalyst shows better long-term stability compared to the commercial catalysts such as Pt_{20}/C or Pt_{40}/C in terms of mass activity and comparable behaviour in terms of specific activity. Normally, PtRu/C catalysts have been considered as the best catalyst due to the bifunctional mechanism of Ru which activates the water molecules at a lower potential than pure Pt (Costamagna and Srinivasan 2001; Schmidt et al. 1997). Steigerwalt et al. developed PtRu/C nanocomposites as anode catalysts for direct methanol fuel cells (Steigerwalt et al. 2002). Gu et al. used PtRu/C nanocomposites for methanol oxidation where I_f/I_b ratio has been calculated as 4.6 (Gu et al. 2014). Chronoamperometric response shows the current density around 0.2 mA cm^{-2} for methanol oxidation at PtRu/C-modified electrodes. Zhu et al. studied the performance of PtRu/C catalysts for methanol oxidation by activation and sensitization treatment where the current density normalized by the Pt loading has been calculated as 0.5 A mg^{-1} (Zhu et al. 2007). All these results derived from Ru-based catalyst are comparable with the newly developed bimetallic Ag@Pt NRDs/L-ERGO catalyst where I_f/I_b ratio is measured as 5 or 12 for ethanol or methanol oxidation.

Conclusions

The challenging task of direct growth of bimetallic Ag@Pt NRDs on L-ERGO nanosheets via galvanic exchange process where Cu acts as sacrificial template was successfully carried out. Here, a facile seed-

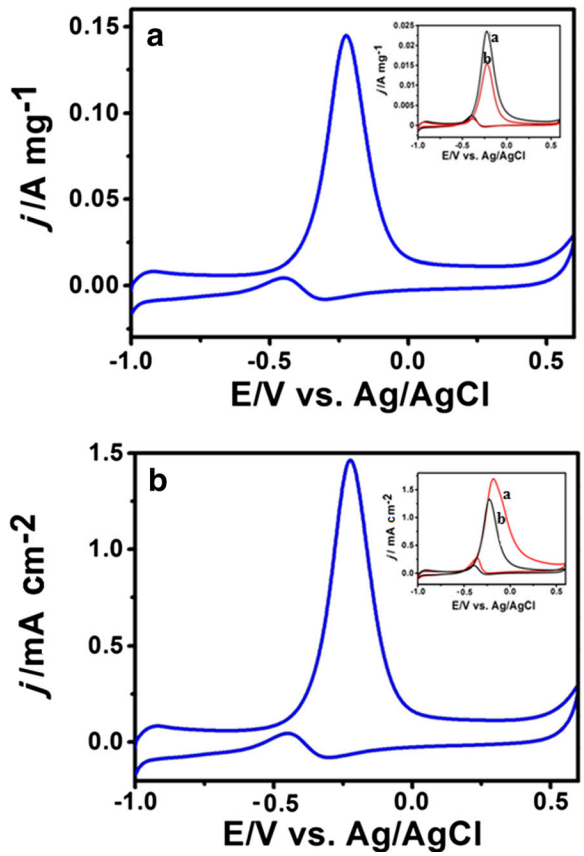

Fig. 8 CV response of mass activity (**a**) and specific activity (**b**) at Ag@Pt NRDs/L-ERGO/GCE for 0.5 M methanol in 0.5 M NaOH at the scan rate of 50 mV s^{-1}. The *insets* in **a** and **b** show CVs of Pt_{20}/C/GCE (*a*) and Pt_{40}/C/GCE (*b*) for methanol oxidation under identical conditions

Table 2 Comparison of onset potential (V), anodic peak potential (V), I_f/I_b ratio, specific activity (mA cm^{-2}) and mass activity (A mg^{-1}) of Ag@Pt NRDs/L-ERGO/GCE with commercial catalysts Pt_{20}/C/GCE and Pt_{40}/C/GCE for methanol oxidation

Catalyst	Onset potential (V)	Anodic peak potential (V)	I_f/I_b	Specific activity (mA cm^{-2})	Mass activity (A mg_{pt}^{-1})
Ag@Pt/L-ERGO	−0.5	−0.24	12	1.48	0.14
Pt_{20}/C	−0.43	−0.2	8.8	1.65	0.023
Pt_{40}/C	−0.43	−0.2	7.4	1.33	0.015

mediated growth followed by electroless galvanic replacement method was introduced for the direct growth of bimetallic Ag@Pt NRDs on L-ERGO nanosheets with ease and confirmed by SEM, EDAX, XRD and Raman spectroscopy. EDAX mapping analysis and CV studies satisfactorily explained the complete replacement of Cu by Pt at Ag surface. The resultant Ag@Pt NRDs/L-ERGO electrode exhibits an excellent electrocatalytic activity and stability for the oxidation of ethanol or methanol in alkaline medium. Importantly, high tolerance level and minimal poisoning effect are observed at Ag@Pt NRDs/L-ERGO-modified electrode which is due to high I_f/I_b ratio towards electrooxidation of ethanol or methanol compared to the commercial catalysts such as Pt_{20}/C and Pt_{40}/C-loaded electrodes. Eventually, the present work arose as a simple, robust method for the development of bimetallic Ag@Pt NRDs/L-ERGO-decorated electrode which could be used as a new generation electrode material in alcohol-based fuel cell applications, catalysis and sensors.

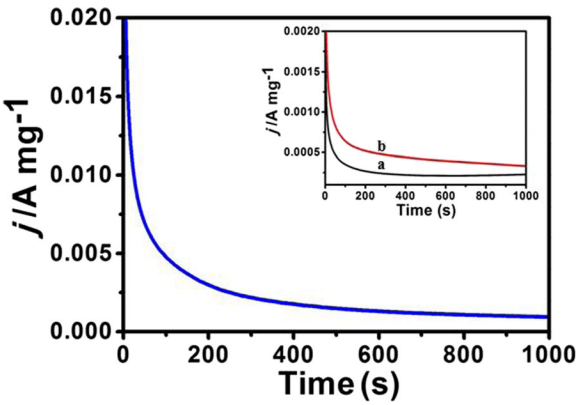

Fig. 9 CA curves of Ag@Pt NRDs/L-ERGO/GCE for 0.5 M methanol in 0.5 M NaOH studied up to 1000 s at −0.4 V. The *inset* shows CA curves of Pt_{20}/C/GCE (*a*) and Pt_{40}/C/GCE (*b*) under identical conditions

Acknowledgements Financial support from DST-SERB, New Delhi (File No. EMR/2015/001893), is gratefully acknowledged. We thank Karunya University, Coimbatore, for providing instrumental facilities.

Compliance with ethical standards

Conflict of interest The authors declare that they have no conflict of interest.

References

Chen A, Hindle PH (2010) Platinum-based nanostructured materials: synthesis, properties, and applications. Chem Rev 110: 3767–3804

Chen J, Wiley B, Lellan JM, Xiong Y, Li ZY, Xia Y (2005) Optical properties of Pd-Ag and Pt-Ag nanoboxes synthesized via galvanic reactions. Nano Lett 5:2058–2062

Chen L, Zhao W, Jiao Y, He X, Wang J, Zhang Y (2007) Characterization of Ag/Pt core-shell nanoparticles by UV–vis absorption, resonance light-scattering techniques, Spectrochim. Acta A 68:484–490

Cheng D, Qiu X, Yu H (2014) Enhancing oxygen reduction reaction activity of Pt-shelled catalysts via subsurface alloying. Phys Chem Chem Phys 16:20377–20381

Costamagna P, Srinivasan S (2001) Quantum jumps in the PEMFC science and technology from the 1960s to the year 2000: part I. Fundamental scientific aspects. J Power Sources 102:242–252

Cui X, Wu S, Jungwirth S, Chen Z, Wang Z, Wang L, Li Y (2013) The deposition of Au–Pt core–shell nanoparticles on reduced graphene oxide and their catalytic activity. Nanotechnology 24:295402 **(10pp)**

Divya P, Ramaprabhu S (2013) Platinum nanoparticles supported on a bi-metal oxide grown carbon nanostructure as an ethanol electrooxidation electrocatalyst. J Mater Chem A 1:13605–13611

Du W, Deskins NA, Su D, Teng X (2012) Iridium–ruthenium alloyed nanoparticles for the ethanol oxidation fuel cell reactions. ACS Catal 2:1226–1231

Easow JS, Selvaraju T (2013) Unzipped catalytic activity of copper in realizing bimetallic Ag@Cu nanowires as a better amperometric H_2O_2 sensor. Electrochim Acta 112:648–654

Feng L, Gao G, Huang P, Wang X, Zhang C, Zhang J, Guo S, Cui D (2011) Preparation of Pt Ag alloy nanoisland/graphene hybrid composites and its high stability and catalytic activity in methanol electro-oxidation. Nanoscale Res Lett 6:551

Gnanaprakasam P, Selvaraju T (2014) Green synthesis of self assembled silver nanowire decorated reduced graphene oxide for efficient nitroarene reduction. RSC Adv 4:24518–24525

Gnanaprakasam P, Jeena SE, Selvaraju T (2015) Hierarchical electroless Pt deposition at Au decorated reduced graphene oxide via galvanic exchanged process: electrocatalytic nanocomposite with enhanced mass activity for methanol and ethanol oxidation. J Mater Chem A 3:18010–18018

Gu J, Liu WC, Zhao ZQ, Lan GX, Zhu W, Zhang YW (2014) Pt/Ru/C nanocomposites for methanol electrooxidation: how Ru nanocrystals surface structure affects catalytic performance of deposited Pt particles. Inorg Chem Front 1:109–117

He W, Wu X, Liu J, Hu X, Zhang K, Hou S, Zhou W, Xie S (2010a) Design of AgM bimetallic alloy nanostructures (M = Au, Pd, Pt) with tunable morphology and peroxidase-like activity. Chem Mater 22:2988–2994

He YB, Li GR, Wang ZL, Ou YN, Tong YX (2010b) Pt nanorods aggregates with enhanced electrocatalytic activity towards methanol oxidation. J Phys Chem C 114:19175–19181

Jeena SE, Gnanaprakasam P, Dakshinamurthy A, Selvaraju T (2015) Tuning the direct growth of Ag_{seeds} into bimetallic Ag@Cu nanorods on surface functionalized electrochemically reduced graphene oxide: enhanced nitrite detection. RSC Adv 5:48236–48245

Kakaei K, Dorraji M (2014) One-pot synthesis of palladium silver nanoparticles decorated reduced graphene oxide and their application for ethanol oxidation in alkaline media. Electrochim Acta 143:207–215

Lee MS, Lee K, Kim SY, Lee H, Park J, Choi KH, Kim HK, Kim DG, Lee DY, Nam SW, Park JU (2013) High-performance, transparent, and stretchable electrodes using graphene−metal nanowire hybrid structures. Nano Lett 13:2814–2821

Liu K, Liu L, Luo Y, Jia D (2012) One-step synthesis of metal nanoparticle decorated graphene by liquid phase exfoliation. J Mater Chem 22:20342–20352

Liu H, Ye F, Yao Q, Cao H, Xie J, Lee JY, Yang J (2014) Stellated Ag-Pt bimetallic nanoparticles: an effective platform for catalytic activity tuning. Sci Rep 4:3969

Luo Z, Yuwen L, Bao B, Tian J, Zhu X, Weng L, Wang L (2012a) One-pot, low-temperature synthesis of branched platinum nanowires/reduced graphene oxide (BPtnw/RGO) hybrids for fuel cells. J Mater Chem 22:7791–7796

Luo B, Liu S, Zhi L (2012b) Chemical approaches toward graphene-based nanomaterials and their applications in energy-related areas. Small 8:630–646

Maiyalagan T, Alaje TO, Scott K (2012) Highly stable Pt-Ru nanoparticles supported on three-dimensional cubic ordered mesoporous carbon (Pt-Ru/CMK-8) as promising electrocatalysts for methanol oxidation. J Phys Chem C 116:2630–2638

Meir N, Plante IJL, Flomin K, Chockler E, Moshofsky B, Diab M, Volokh M, Mokari T (2013) Studying the chemical, optical and catalytic properties of noble metal (pt, Pd, Ag, Au)–Cu_2O core–shell nanostructures grown via a general approach. J Mater Chem A 1:1763–1769

Nguyen TGH, Pham TVA, Phuong TX, Lam TXB, Tran VM, Nguyen TPT (2013) Nano-Pt/C electrocatalysts: synthesis and activity for alcohol oxidation. Adv Nat Sci: Nanosci Nanotechnol 4:035008 **(8pp)**

Peng C, Liu M, Hu Y, Yang W, Guo J, Zheng Y (2015) Pd*x*Ag*y* alloy nanoparticles supported on reduced graphene oxide as efficient electrocatalyst for ethanol oxidation in alkaline medium. RSC Adv 5:49899–49903

Rashid M, Jun TS, Jung Y, Kim YS (2015) Bimetallic core–shell Ag@Pt nanoparticle-decorated MWNT electrodes for amperometric H_2 sensors and direct methanol fuel cells. Sensor Actuat B-Chem 208:7–13

Safavi A, Kazemi H, Momeni S, Tohidi M, Mehrin PK (2013) Facile electrocatalytic oxidation of ethanol using Ag/Pd nano alloys modified carbon ionic liquid electrode. Int J Hydrogen Energ 38:3380–3386

Schmidt TJ, Noeske M, Gasteiger HA, Behm RJ, Britz P, Brijoux W, Bonnemann H (1997) Electrocatalytic activity of PtRu alloy colloids for CO and CO/H_2 electrooxidation: stripping voltammetry and rotating disk measurements. Langmuir 13:2591–2597

Sharma S, Ganguly A, Papakonstantinou P, Miao X, Li M, Hutchison JL, Delichatsios M, Ukleja S (2010) Rapid microwave synthesis of CO tolerant reduced graphene oxide-supported platinum electrocatalysts for oxidation of methanol. J Phys Chem C 114:19459–19466

Shen Y, Zhang Z, Long R, Xiao K, Xi J (2014) Synthesis of ultrafine Pt nanoparticles stabilized by pristine graphene nanosheets for electro-oxidation of methanol. ACS Appl Mater Interfaces 6:15162–15170

Steigerwalt ES, Deluga GA, Lukehart CM (2002) Pt-Ru/carbon fiber nanocomposites: synthesis, characterization, and performance as anode catalysts of direct methanol fuel cells. A search for exceptional performance. J Phys Chem B 106:760–766

Tedsree K, Li T, Jones S, Chan CWA, Yu KMK, Bagot PAJ, Marquis EA, Smith GDW, Tsang SCE (2011) Hydrogen production from formic acid decomposition at room temperature using a Ag–Pd core–shell nanocatalyst. Nat Nanotechnol 6:302–307

Wang RX, Fan JJ, Fan YJ, Zhong JP, Wang L, Sun SG, Shen XC (2014) Platinum nanoparticles on porphyrin functionalised graphene nanosheets as a superior catalyst for methanol electrooxidation. Nanoscale 6:14999–15007

Wojtysiak S, Solla-Gullón J, Dłu˙zewskic P, Kudelski A (2014) Synthesis of core–shell silver–platinum nanoparticles, improving shell integrity. Colloid Surf A 441:178–183

Xi J, Wang J, Yu L, Qiu X, Chen L (2007) Facile approach to enhance the Pt utilization and CO-tolerance of Pt/C catalysts by physically mixing with transition-metal oxide nanoparticles. Chem Commum 16:1656–1658

Xie S, Jin M, Tao J, Wang Y, Xie Z, Zhu Y, Xia Y (2012) Synthesis and characterization of $Pd@M_xCu_{1-x}$(M = Au, Pd, and Pt) nanocages with porous walls and a yolk–shell structure through galvanic replacement reactions. Chem Eur J 18:14974–14980

Xu C, Liu Y, Wang J, Geng H, Qiu H (2011) Fabrication of nanoporous Cu–Pt(Pd) core/shell structure by galvanic

replacement and its application in electrocatalysis. ACS Appl Mater Interfaces 3:4626–4632

Zeng J, Yang J, Lee JY, Zhou W (2006) Preparation of carbon-supported core-shell Au-Pt nanoparticles for methanol oxidation reaction: the promotional effect of the Au core. J Phys Chem B 110:24606–24611

Zeng M, Wang H, Zhao C, Wei J, Wang W, Bai X (2015) 3D graphene foam-supported cobalt phosphate and borate electrocatalysts for high-efficiency water oxidation. Sci Bull 60:1426–1433

Zhang W, Yang J, Lu X (2012) Tailoring galvanic replacement reaction for the preparation of Pt/Ag bimetallic hollow nanostructures with controlled number of voids. ACS Nano 6: 7397–7405

Zhang L, Iyyamperumal R, Yancey DF, Crooks RM, Henkelman G (2013) Design of Pt-Shell nanoparticles with alloy cores for the oxygen reduction reaction. ACS Nano 7:9168–9172

Zhu J, Su Y, Cheng F, Chen J (2007) Improving the performance of PtRu/C catalysts for methanol oxidation by sensitization and activation treatment. J Power Sources 166:331–336